Development of Open-Cell Ni–Ti Foams Fabricated via Powder Metallurgy using NH_4HCO_3 as a space holder

[a]Ajay Kumar Barnwal, [b]Dr. Hemant Jain and [c] Dr. Parveen Kumar
a-Research Scholar, Capital University, Koderma, Jharkhand
b-Supervisor, Dr. Hemant Jain, Associate Professor, Capital University, Koderma, Jharkhand
c-Co-Supervisor, Dr. Parveen Kumar, Associate Professor, Department of Industrial & Production Engineering, Guru Ghasidas Vishwavidyalaya, Bilaspur

Abstract
Ni-Ti-foams were made using evaporative types of space holders such as ammonium bicarbonate (ABC) with a wide range of porosities (55 to 89%) through powder metallurgy techniques. The green compacted pellets, after evaporation of $NH_4(HCO_3)$,were sintered at 1100ºC for 2 hrs. The XRD and EDX analysis confirms that there is no residual space holder. The extent of openness of cell walls increases with increase in porosity. The compressive stress-strain behavior of these foams varies with the relative density. The peak stress and energy absorption of these foam increases with relative density following power law and linear relationships respectively, and the densification strain decreases with relative density following a linear relationship.

Key Words: Ni-Ti foams, Plateau Stress, Densification strain, Compressive deformation behavior.

Introduction

A rare combination of properties, including high strength under static and dynamic loading conditions, reasonably good ductility, fracture toughness, moderate stiffness, excellent corrosion resistance, and good shape memory effect, are displayed by NiTi (Nitinol) alloy, which has a nearly equiatomic composition of Ni and Ti [1–3]. Due to these special qualities, this alloy can be regarded as a multifunctional material and is utilized in the following fields: (i) materials with high energy absorption and damping [1–3], (ii) actuators and sensors [4], and (iii) bio-implants [5-7]. This alloy outperforms Ti and other alloys due to its shape memory effect, low stiffness, and bioinertness [5-7]. This alloy is useful for actuators and sensors due to its shape recovery capabilities as a function of temperature and load [1-4]. Since the deformation stress, modulus, and heat transmission ability of foams change with the porosity percentage, altering the porosities within the materials might alter the biocompatibility as well as the shape recovery rate [8–10]. These foams' superior qualities make them suitable for use in bone implants. By altering its porosity, the bone implant's strength and modulus can be changed [10–12]. The size and location of the pores in the foam can be adjusted to influence the architecture of the bone implant [13]. In a similar vein, altering the foam's cell size and openness can regulate heat transfer. As a result, one can carefully modify the pore's size, openness, and volume fraction to suit the implant's needs. Given the aforementioned, a lot of effort is being put into creating Ni-Ti foams and describing their mechanical and architectural characteristics [10–13, 14–21]. Making Ni-Ti foam via the melt technique is challenging because of the metal's high air reactivity, liquid Ni-Ti's high reactivity to commonly employed crucible materials, and its high melting temperature (1339ºC) [10–13]. According to the published literature, Ni-Ti foams can be produced using a variety of powder metallurgy-based techniques. These procedures are mainly divided into (i) partial powder sintering [14], (ii) complete densification of Ni-Ti powder (cold and hot compaction), followed by the expansion of trapped gas during densification [11–13], (iii) sintering with spark plasma [22], (iv] sintering and then removing the space holder after densifying the space holder and Ni-Ti powder mixture [10,13,16,23,24], and (v) combustion sintering (Self propagating High temperature Synthesis, or SHS) [19,21]. The methods of gas expansion, spark plasma sintering, and partial powder sintering are not appropriate for obtaining controlled cell size and a high degree of porosity. When the SHS approach is used to create Ni-Ti foams, the reported cell sizes are not consistent [19, 21]. The restrictions of other processes can be solved by using the space holder technique. In Ni-Ti foam, the size, shape, distribution, and volume percentage of porosity can be carefully controlled by adjusting the size, shape, distribution and space holder volume fraction [16, 23, 24]. Numerous researchers have employed the SHS technique to create Ni-Ti foam, however they have discovered that this method has a high degree of inhomogeneous cell size distribution and produces a significant number of intermetallics. Various metallic foams have been made using various types of space holders.

However, NaF and NaCl have been employed as space holders mainly for the production of Ni-Ti foams [10, 13, 24, 25]. Because of their high melting points, which enable the hot compacting of Ni-Ti and NaF/NaCl powder mixes at high temperatures, where partial sintering would occur, NaF and NaCl were chosen. However, hot isostatic pressing or hot compaction raises the price and improves the product expense. There have been very few attempts to create very porous Ni-Ti foam with NH4(HCO3) acting as a space holder, but [23]. The Ni-Ti foam's highly uneven cell size distribution was caused by the large range of NH4(HCO3) particle sizes (200–500 µm) used in its production. It is crucial to use space holders with a limited size range in order to ensure uniform cell size. Rare earth metals like Nb have been used in pre-alloyed Ni-Ti powder for liquid stage sintering at lower temperatures in an attempt to create Ni-Ti foam. Additionally, a portion of the cell wall pores in the extremely porous Ni-Ti foam have been closed to improve its strength and modulus [24]. Likewise, Cu was used with Ni-Ti powder to reduce the temperature during liquid phase sintering and to increase modulus and strength [26]. NH4(HCO3) was used as a space holder in certain situations to create Ti-foams [27]. Its ability to evaporate at very low temperatures (between 100 and 150 oC) without reacting with base materials like Ni or Ti is one of its advantages. When the temperature is right, this porous compact can be sintered. Avoid sintering at temperatures close to liquids and over extended periods of time in order to manage cell size shrinkage. There were no systematic investigations conducted to evaluate the porosity and cell size distribution of the Ni-Ti foam at different NH4(HCO3) particle volume and size fractions. By employing NH4(HCO3) as a space holder in different amounts, the current study seeks to evaluate the porosity fraction and micro-architectural features of Ni-Ti foams before characterizing these foams in terms of their microstructure and mechanical attributes. The synthesised Ni-Ti foams' elastic recovery strain has also been studied in relation to their porosity fraction and degree of deformation.

2. Experimental Procedure

2.1 Material Preparation

Pure 99.0% pre-alloyed equiatomic Ni-Ti powder (50:50) from NANOSHEL, U.S.A., was utilized as the parent material. Particles of Ni-Ti powder ranged in size from 1 to 10 µm on average. Ammonium bicarbonate $NH_4(HCO_3)$ particles with a cubical form and an average size of 285±10µm have been employed as space holders. Alfa Aesar, U.K., provided the NH4(HCO3) particles. Cold-compacted pallets were given green strength using a Poly Vinyl Alcohol (PVA) solution, an organic binder (5 Wt% PVA and 95 Wt% water). Figure 1(a) and Figure 1(b) display the size distribution of NH4(HCO3) and Ni-Ti powders, respectively.

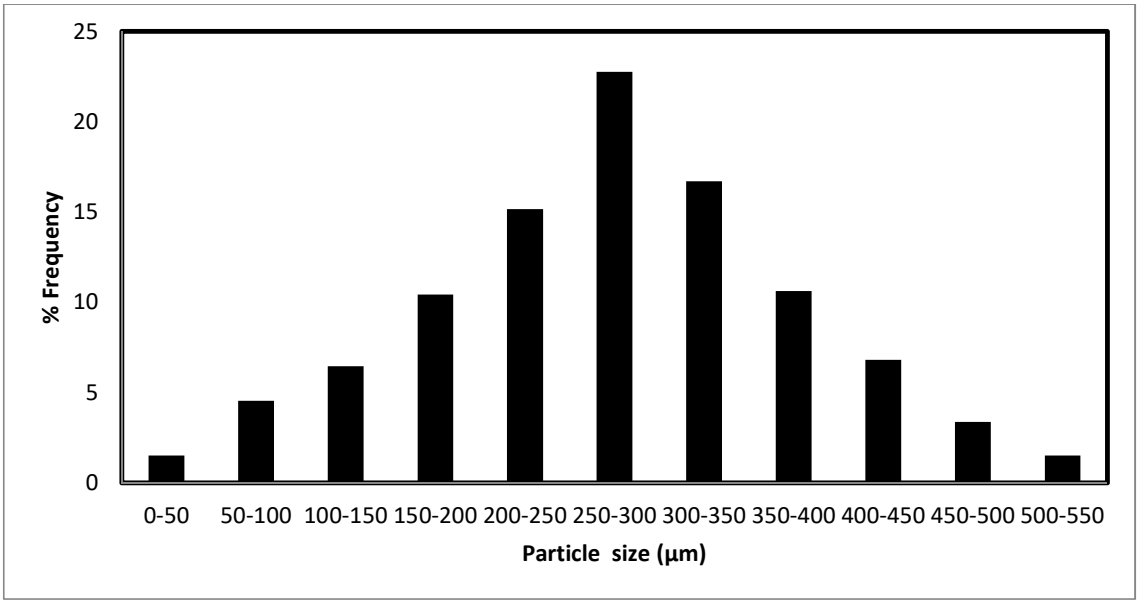

(a)

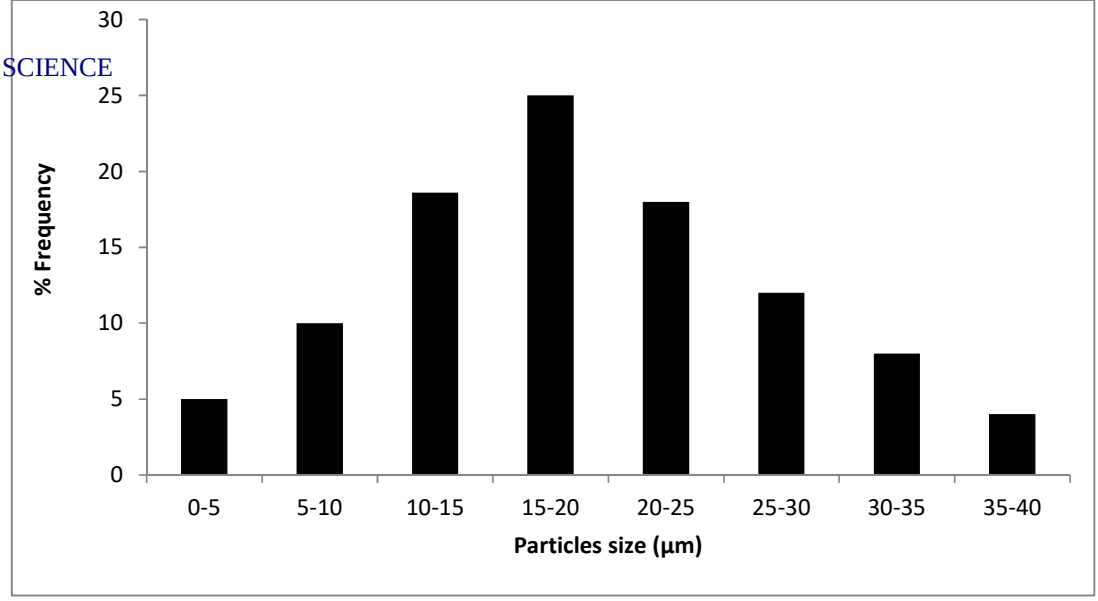

(b)

Fig. 1: Size distribution of (a) ammonium bi-carbonate powder and (b) Ni-Ti powder

2.2 Foam Production

Ni-Ti powder (50–80%) and NH4 (HCO3) powder were mixed in different proportions as a space holder. An organic binder made of PVA solution was added to this mixture. The powder mixture was cold compressed at 200 MPa in a cylindrical die with a diameter of 15 mm in a 40-ton hydraulic press.
To get the appropriate porosities, several concentrations of Ni-Ti powder and NH4(HCO3) were used. The amount of Ni-Ti powder and NH4(HCO3) was calculated using the following relationship:

$$\frac{W_{SS}}{W_{SP}} = \frac{\rho_{ss}(1-V_{SP})}{(\rho_{sp}*V_{sp})} \quad \text{..... (i)}$$

where Wss stands for Ni-Ti weight, Wsp for NH4(HCO3) weight, ρ_{ss} for Ni-Ti powder density, ρ_{sp} for space holder density, and Vsp for space holder volume fraction. Despite the fact that $NH_4(HCO_3)$ melts at 41.9ºC, the cold compacts were heated to 200ºC for four hours to ensure that all space-holding particles were eliminated. To completely remove the organic binder, or PVA, these pellets were dried and then heated to 400–500 degrees Celsius for two hours.

. These samples were therefore sintered for two hours at $11{,}00^0$ C under 10^{-4} mbar of vacuum. Fig. 2(a) shows the flowchart for creating Ni-Ti foam. Fig. 2(b) displays samples of sintered foam.

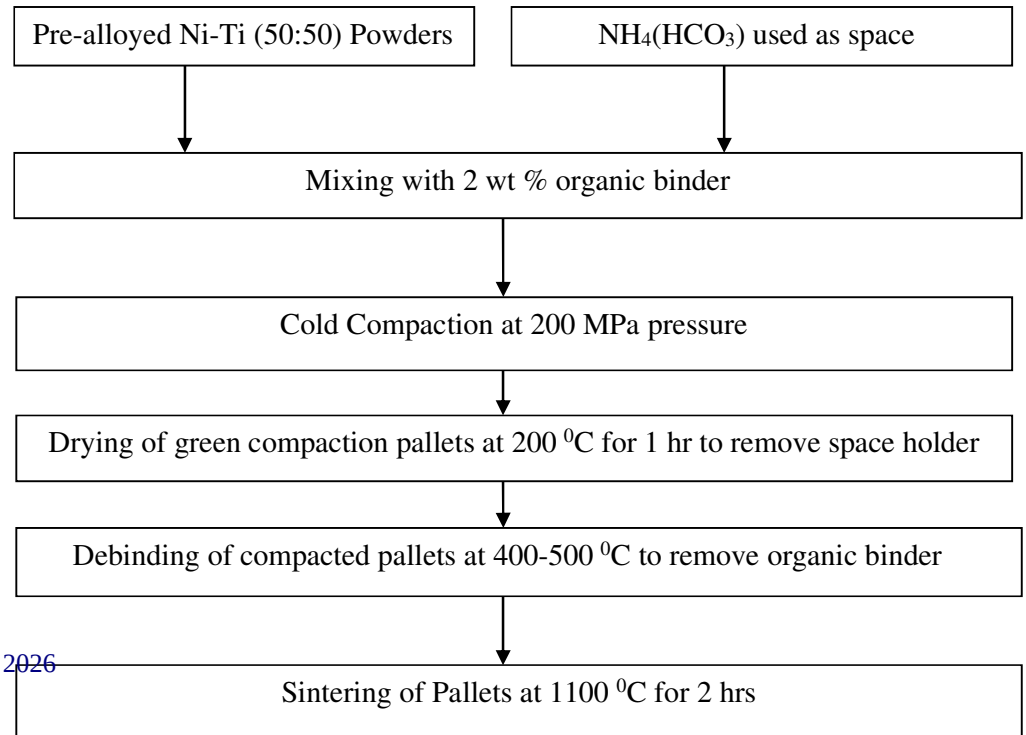

(a)

(b)

Fig. 2: (a) Flow sheet diagram for making Ni-Ti foam and (b) Sintered Ni-Ti foam samples

2.3 Microstructural Characterization

Scanning electron microscopy (SEM) (JEOL: Model: 5600) was used to examine the microstructure of Ni-Ti foams, and an energy dispersive X-ray analyzer (Model IE Synergy 250) was utilized to ascertain the chemical composition of the ingredients. Cell size and cell wall thickness were measured using SEM micrographs. To measure the cell size and cell wall thickness, about 100 cells were randomly selected.
Pre-alloyed powder and sintered foams were subjected to X-ray diffraction analysis using an X-ray diffractometer (Bruker-D8 model with Cuα radiation). To determine the phases present in the cell wall, the diffraction patterns were recorded at a scan rate of 0.010 min^{-1} while operating at 30 kV and 40 mA.

2.4 Compression Test

At CSIR-AMPRI Bhopal, cylindrical samples of sintered Ni-Ti foam (15 mm in diameter and 10 mm in height) were subjected to compression tests at room temperature with different strain rates (0.001, 0.01, 0.1, and 1.0 /s) using the Universal Testing Machine (Instron model no.8801). The stress-strain curves of several foam samples were recorded. The plateau stress, densification strain, and energy absorption were determined using the compressive stress-strain plot and conventional methods [27]. The loading and unloading cycles of selected foam samples at room temperature are performed using the same UTM.

3. Results and Discussions

3.1 Materials and Microstructures

The microstructures of Ni-Ti foams with varying porosities are shown in Figure 3. Figure 3(a) depicts the microstructure of Ni-Ti foam with a relative density of 0.38. It has been observed that each cell's pores range in size from 226 to 224 µm and have a somewhat oval shape. The average thickness of the cell wall is 95 ± 10 µm. Figure 3(b) depicts the microstructure of Ni-Ti foam with a relative density of 0.31. It also reveals that the cells are elliptical in shape and have an average size of roughly 227 ± 15 µm. Figs. 3(c) and 3(d) show the microstructure of Ni-Ti foam with relative densities of 0.25 and 0.21, respectively.
With average diameters of 234 ± 15 µm and 229 ± 15 µm, respectively, the cells in both microstructures are likewise demonstrated to have a somewhat elliptical shape. It is observed that the cell widths are almost independent of the relative density.
But as the relative density decreases, the cell wall's thickness also decreases. This is due to the fact that the size of $NH_4(HCO_3)$, which is used as a space holder, and the sintering temperature (1100ºC) remained consistent for all varieties of Ni-Ti foam. In this study, the average size of $NH_4(HCO_3)$ was 235 ± 10 µm. The foam samples under study had cell diameters ranging from 225 to 234 µm.

This indicates that just a small amount of shrinking (5 to 10%) has occurred when compared to the cell size for green compacts (~240 µm ± 15 µm). For foam samples, the difference between the volume fraction of $NH_4(HCO_3)$ and the total volume of compact is somewhat greater than the overall relative density, or [1-vol. percent of $NH_4(HCO_3)$]. This is due to the substantial amount of micro-porosity (between 15% and 20%) present in the cell walls. The connections between neighbouring cells and the micro-porosities in the cell wall are depicted in Fig. 3(e).

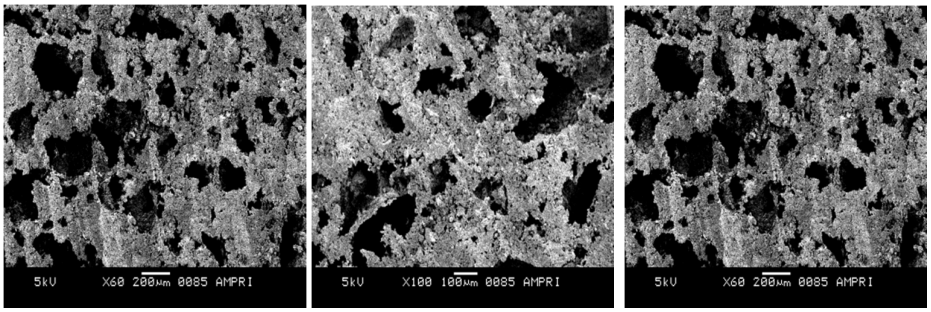

(a) ρ_{rd} =0.38 (b) ρ_{rd} =0.31 (c) ρ_{rd} =0..25

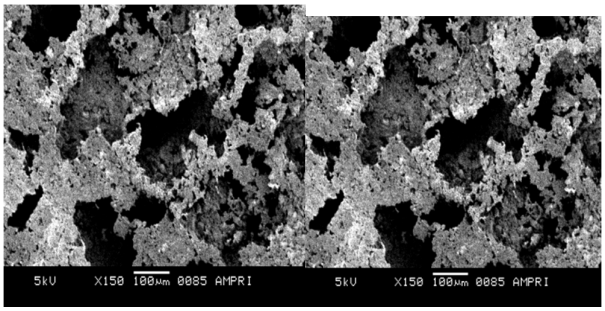

(d) ρ_{rd} =0.22 (e) micro-porosity

Fig. 3: Microstructures (a) ρ_{rd} =0.38 (b) ρ_{rd} =0.31 (c) ρ_{rd} =0.25 (d) ρ_{rd} =0.22 (e) higher magnification micrograph showing microporosities in cell wall

3.2 EDX and XRD analysis

The EDX studies of the foam samples for different relative densities are shown in Figure 4. The bulk of the Ni-Ti foam is found to consist of Ni and Ti, with traces of additional elements. The majority of the other elements are oxygen due to the oxidation of Ni-Ti at high temperatures. Other components may become trapped during processing, such as compaction, sintering, polishing, etc. It is evident from Figure 4 that EDX patterns are almost independent of the relative density of the foam.

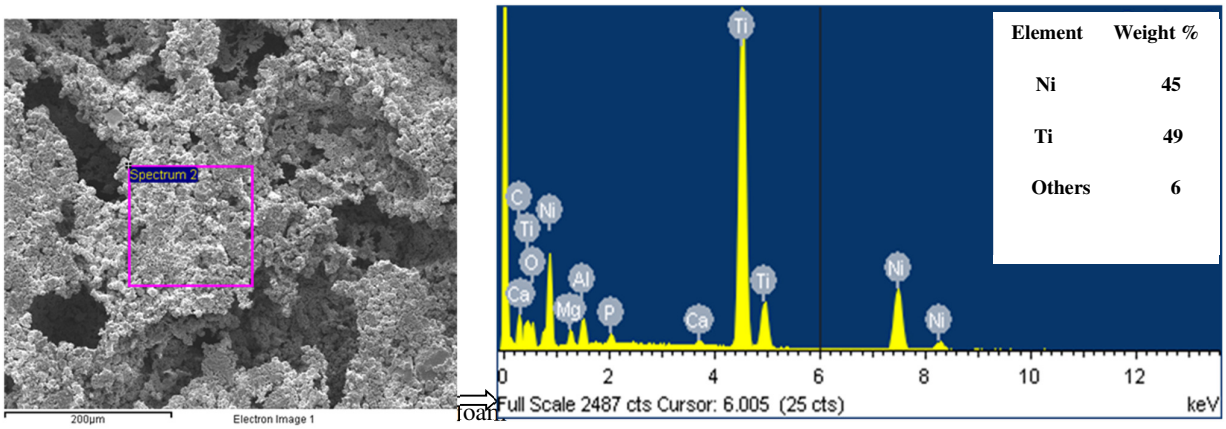

foam.

Microporosity and other impurities may affect these foams' deformation response. The XRD patterns of the sintered Ni-Ti foams and the Ni-Ti powder mix are shown in Figures 5(a) and 5(b), respectively. It is clear from these figures. These materials are mostly composed of Ni-Ti, with trace quantities of Ni_3Ti and Ni and Ti oxides. These foams, which are made of Ni and Ti, may exhibit pseudo elastic recovery due to the shape memory effect.

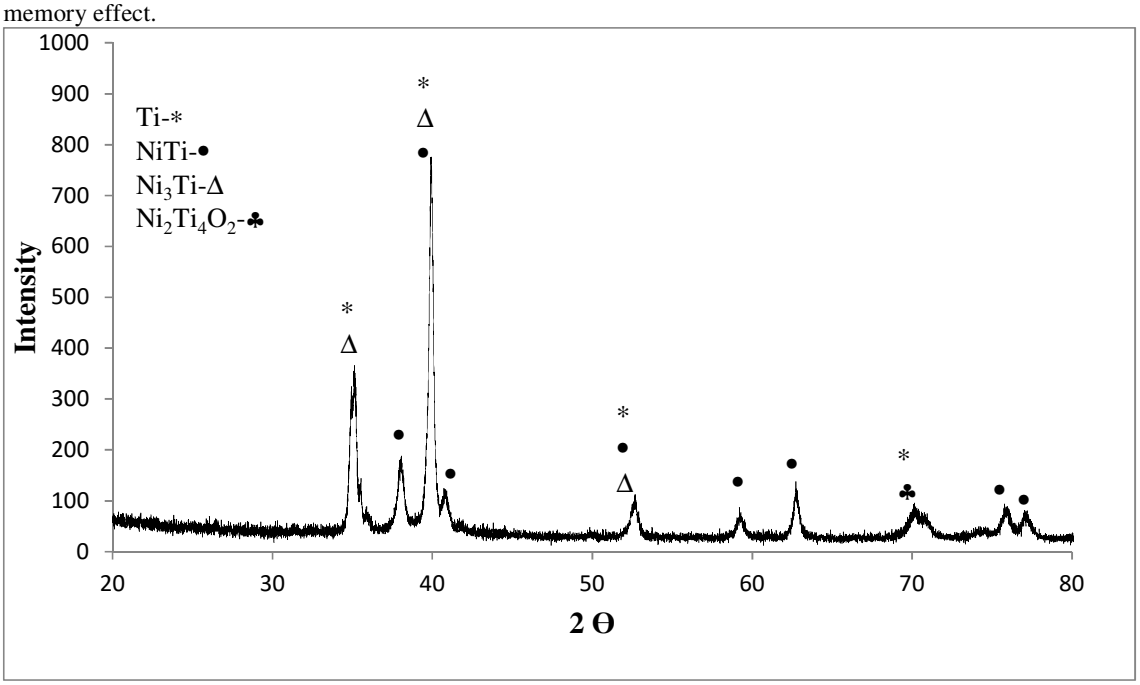

(a)

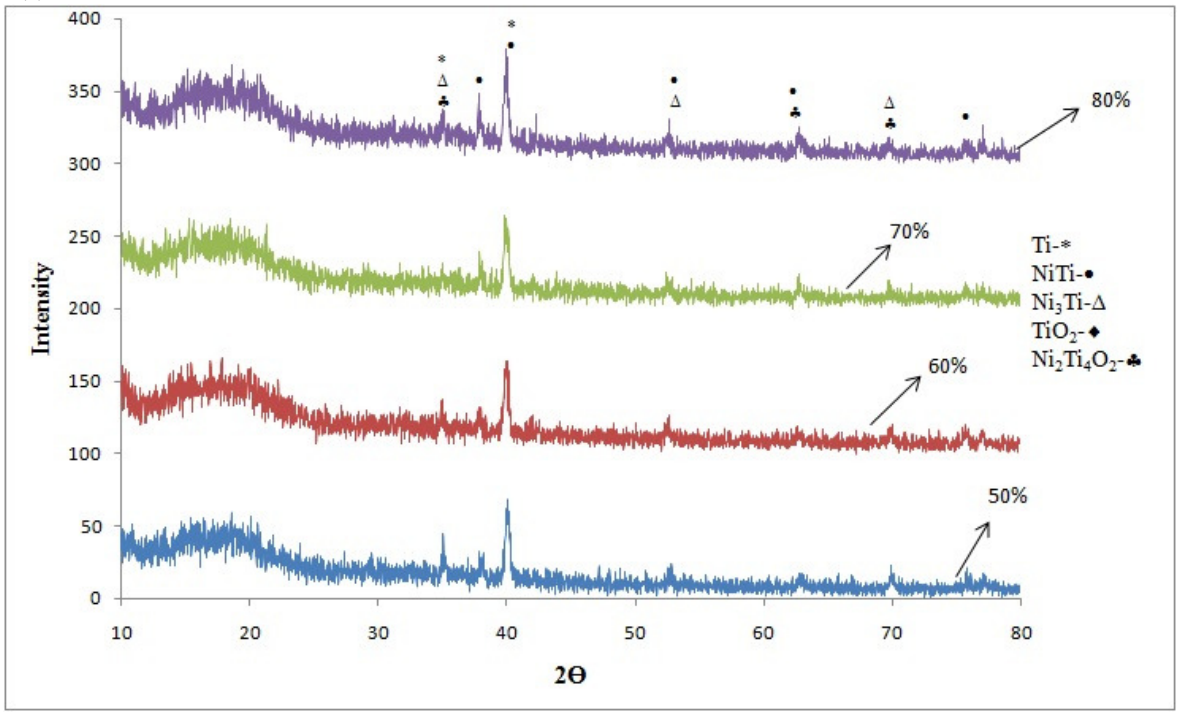

It is important to note that the stress-strain curves displayed strain hardening behavior at rd between 0.31 and 0.34. However, there is no indication of strain hardening at lower rd. The main cause of this is increased porosity at low rd, which lessens strain during hardening. In this instance, we took into account the peak stress

or yield stress in place of the plateau stress. To investigate the impact of these factors on the strength of such foams, these stresses are displayed as a function of strain rate and relative density. Furthermore, it has been shown that permanent yielding has been seen for the majority of foam samples beyond 0.1 strain. The strain at which the stress grows stiffly with additional strain after reaching the valley region is known as the densification strain. The area under the stress-strain curves, taking into account strain up to 0.5, is used to compute the energy absorption of these foams.

3.3 Compressive stress-strain behaviour

Figure 6 shows the compressive stress-strain diagram of Ni-Ti foams of different relative densities at fixed strain rate 0.01/s. From this figure it is clear that the relative density (rd) affects the type of stress-strain curve. The stress –strain diagram of Ni-Ti foam at 0.01 strain rate with different relative densities shows three distinct regions: (i) a linear region, (ii) a plateau region, and (iii) a densification region.

When foam had a higher relative density, the stress rose gradually until it reached the densification stage, at which point it rapidly dropped to a minimum. The stress remained constant until the densification area after reaching a high value and slightly decreasing at intermediate rd [0.21 < rd < 0.38].
This may be due to the fact that these three relative density regimes have different deformation mechanisms. Cell wall shearing is the main cause of the cell wall's brittle nature at higher rd. At lower rd, the cell wall displays ductile activity through some kind of bending and softening. The middle range exhibits both ductile and brittle characteristics. The stress-strain curves showed strain hardening behavior at rd between 0.31 and 0.38, which is significant. At lower rd, there is no sign of strain hardening, nevertheless.

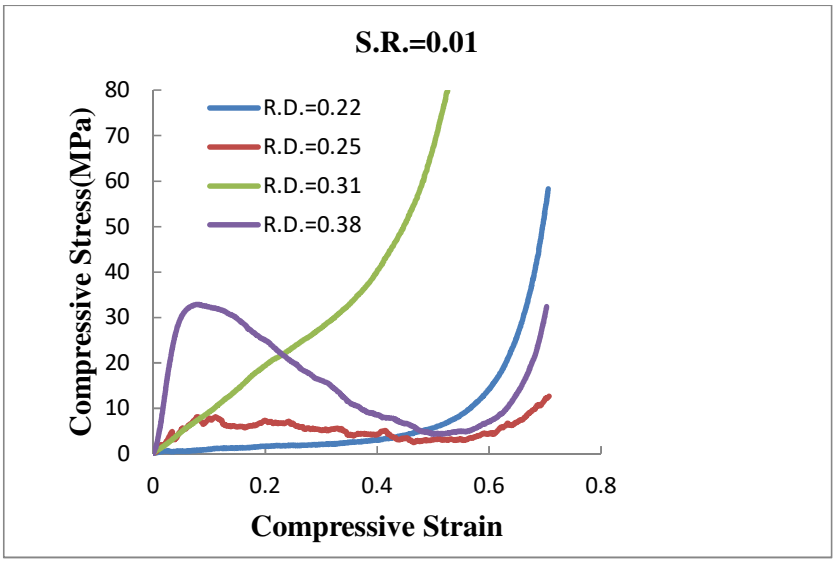

Fig 6: Compressive stress-strain diagram of different relative density at S.R.=0.01m/s

3.4 Plateau Stress

The Plateau stress σ_{Pl} as a function of relative density for Ni-Ti foam with different relative density with ABC is shown in figure 7. From figure it is clear that plateau stress increases with increase in relative density. It is noted that the σ_{Pl} follows power law relationship with relative density like reported for other foams in literature [34-41]. The co-efficient and exponent of the power law relations as shown in equation

$\sigma_{Pl} = 28275x^{6.473}$ …….. (ii)

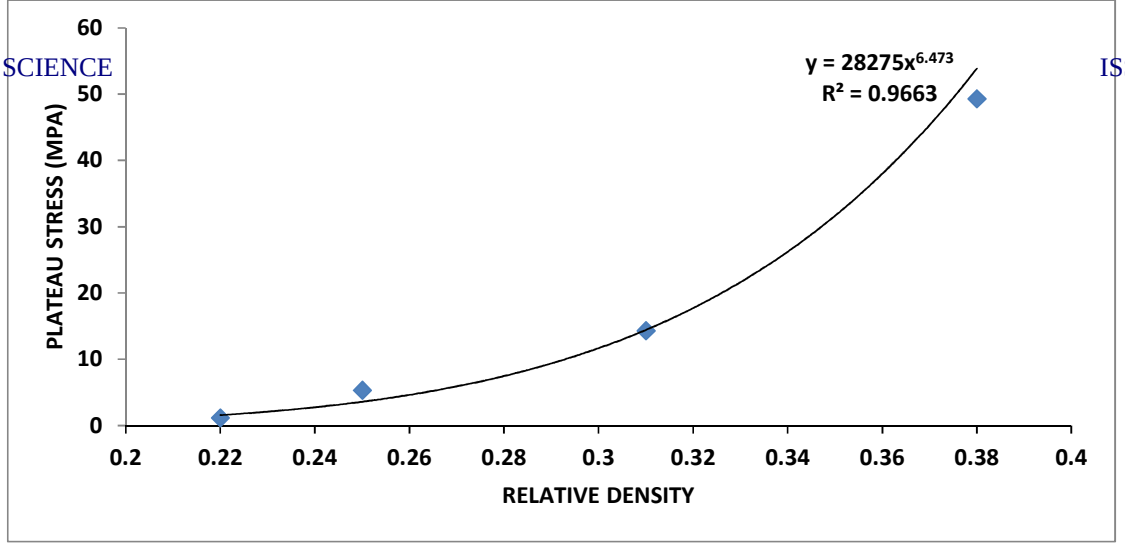

Fig 7: Plateau Stress Vs relative density at S.R.=0.01m/s

3.4 Densification strain

The Densification strain ε_d as a function of relative density for Ni-Ti foam with different relative density with ABC is shown in figure 8. From figure it is clear that ε_d decreases with increase in relative density. is noted that the ε_d follows linear relationship with relative density like reported for other foams in literature [34-41]. The co-efficient and exponent of the linear relation as shown in equation

ε_d = -0.4467x + 0.6495 ..... (iii)

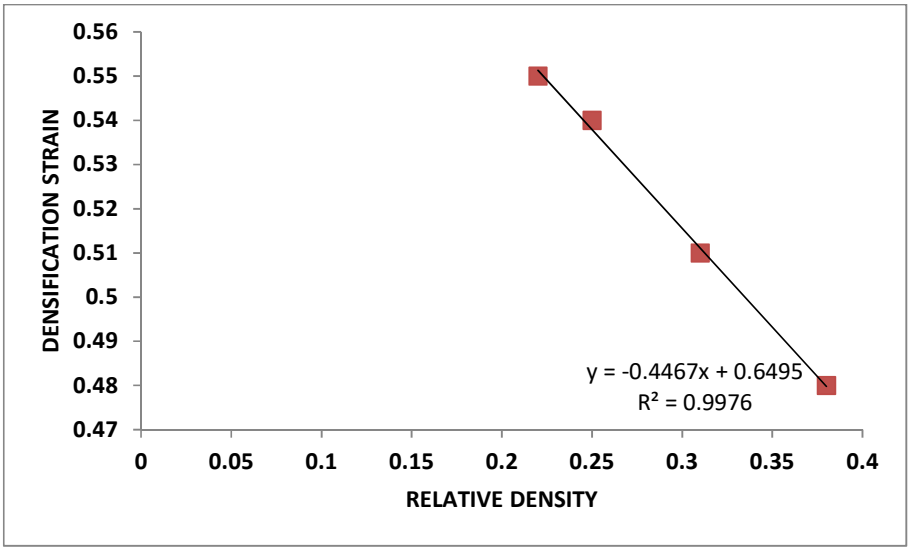

Fig 8: Densification Strain Vs relative density at S.R.=0.01m/s

4. Conclusions

The present investigation yields the following findings:
(i) Ammonium-bicarbonate NH4(HCO3) can be used as a space holder in powder metallurgy to produce Ni-Ti foam.

(ii) Cell sizes and relative densities are almost constant. Nevertheless, the cell wall's thickness decreases along with the relative density. The cells, which range from 5 to 10%, are smaller than the space holder.

(iii) According to a power law and a linear relationship, respectively, the plateau stress and energy absorption increase as relative density increases. The densification strain decreases and shows a linear connection as the relative density increases. A correlation between strain rate and relative density as well as the plateau stress, energy absorption, and densification strain is formed by the empirical relationships found within the designated range.

(iv) Research that has been published indicates that Ni-Ti foams are more sensitive to strain rate than Al and Ti foams. This is due to the Ni-Ti matrix's increased sensitivity to strain rate.

References

1. K. Otsuka and C.M. Wayman, Shape memory materials. Cambridge, New York, Cambridge University Press; 1998.
2. Ying Zhao, Minoru Taya and Hiroshi Izui, Study on energy absorbing composite structure made of concentric NiTi spring and porous NiTi, Int. J. Solids Struct. 43(2006) 2497-2512.
3. Muhammad A Qidwai, Virginia G DeGiorgi, Numerical assessment of the dynamic behavior of shape memory alloy composite, Smart Mater. Struct. 13 (2004) 134-145.
4. Dana M. Elzay, Aarash Y.N.Sofia and Haydn N.G. Wadley, A shape memory based multifunctional structural actuator panel, Int. J. Solids Struct. 42 (2005) 1943-1955.
5. Seung-Baik Kang, Kang-Sup Yoon, Ji-Soon Kim, Tae-Hyun Nam and Victor E. Gjunter, In vivo results of porous Ti-Ni shape memory alloy: bone response and growth, Mater. Trans. 43 (2002) 1045-1048.
6. Lorenza Petrini and Francesco Migliavacca, Biomedical applications of shape memory alloys". J. Metallurgy, doi:10.1155/2011/501483
7. Daniela Tarnită, D. N. Tarnită, N. Bizdoacă, I. Mindrilă and Mirela Vasilescu, Properties and medical applications of shape memory alloys, Romanian J. Morphology and Embriology 50 (1) (2009) 15-21.
8. S. Rhalmi, M.Odin, M. Assad, M. Tabrizian, C.H.Rivard, L.H.Yahia, Hard soft tissue and invitro cell response of nickel titanium: a biocompatibility evaluation, Biomed. Mater. Eng. 9 (1999):151-62.
9. R.A. Ayers, S.J.Simske, T.A.Batman, A.Petkus, R.L.C Sachdeva and V.E.Gyunter, Effect of nitinol implant porosity on cranial bone ingrowth and apposition after 6 weeks, J. Biomed mater. Res. 45 (1999) 42-47.
10. Ampika Bansiddhi and David C. Dunand, Shape memory Ni-Ti foams produced by solid state replication with NaF, Intermetallics 15 (2007) 1612-1622.
11. Christian Greiner, Scott M. Oppenheimer and David C. Dunand, High strength, low stiffness, porous NiTi with superelastic properties, David C Dunand, Acta Biomateri. 1 (2005) 705-716.
12. A. Bansiddhi, T.D.sargeant, S.I.Stupp and D.C.Dunand, Porous NiTi for bone implants: A review, Acta Biomater, 4 (2008) 773-82.
13. A. Bansiddhi and D.C. Dunand, Shape-memory NiTi foams produced by replication of NaCl space-holders, Acta Biomaterialia 4 (2008) 1996-2007.

14. B. Yuan, X P Zhang, C Y chung, M.Q. Zeng. M. Zhu, A comparative study of the porous TiNi shape memory alloys fabricated by three different processes, Metall. Mater. Trans. A 37A (2006) 755-760.

15. B. Bertheville**,** Porous single-phase NiTi processed under Ca reducing vapor for use as a bone graft substitute, Biomaterials 27 (2006) 1246.

16. Tarik Aydog˘ Mus¸ and S¸akir Bor, Enhanced sintering of TiNi shape memory foams under Mg vapour atmosphere, Metall. Mater. Trans. A 43A (2012) 5173-5180.

17. S. K. Sadrnezhadd, H. Arami, H. Keivan and R. Khalifezadeh, Powder Metallurgical Fabrication and Characterization of Nanostructured Porous NiTi Shape Memory Alloy, Mater. Manuf. Process 21 (2006) 727-735.

18. Anselm J. Neurohr and D. C. Dunand, Mechanical anisotropy of shape memory NiTi with two dimensional networks of microchannels, Acta mater. 59 (2011) 4616-4630.

19. Yuya Arakawa, Makoto Kobashi and Naoyuki Kanetake, Effect of Elemental powder size on foaming behavior of NiTi alloy made by Combustion shynthesis, Materials 5 (2012) 1267-1274.

20. Shuilin Wua, Xiangmei Liu,K.W.K. Yeung, Tao Hu, Zushun Xu, Jonathan C.Y. Chung b, and Paul K. Chu , Hydrogen release from titanium hydride in foaming of orthopedic NiTi scaffolds, Acta Biomater. 7 (2011) 1387-1397.

21. P. Bassani, E.Bassani, A. Tuissi, P. Giuliani and C. Zanotti, Nonequiatomic NiTi alloy Produced by self propagating high temperature synthesis, J. Mater. Eng. Perf. 23(2014) 2373-2378.

22. Y Zhao, M. Taya, Y.S. Kanga and A. Kawasaki, Compression behavior of porous NiTi shape memory alloy, Acta mater. 53 (2005) 337-343.

23. J.Y.Xiong, Y.C.Li, X.J.Wang, P.D.Hodgsona and C.E.Wen, Titanium Nickel shape memory alloy foams for bone tissue engineering, J. Mechanical Behv. Biomed. Mater. 1 (2008) 269-273.

24. A Bansiddhi and D.C. Dunana, Processing of Ni-Ti foams by Transient Liquid phase sintering., J. Mater. Eng Perf. 20 (2011) 511-516.

25. X.K.jhao, H.B.Sun, L.Lan, J.H.huang, H.Zhang and Y.Wang, Pore structures of high-porosity NiTi alloys made from elemental powders with NaCl temporary space-holders, Mater. Lett. 63 (2009) 2402-2404.

26. M. L. Young, J.D. deFouw, J. Frenzel and D.C.Dunand, Cast replicated NiTiCu foams with superelastic properties, Metall. Mater. Trans. A 43A (2012) 2939-2944.

27. D.P Mondal, Mahesh Patel, S. Das, A.K. Jha, Hemant Jain, G. Gupta,and S.B Arya, Titanium foam with coarser cell size and wide range of porosity using different types of evaporative space holder through powder metallurgy, Mater. Des. 63 (2014) 89-99.

28. A. Paul and U. Ramamurty. Strain rate sensitivity of a closed-cell aluminium foam, Mater. Sci. Eng. A 281 (2000) 1-7.

29. Lee Sungsoo, Barthelat Francois, Moldovan Nicolaie, D.Espinosa Horacio and N.G Waldley Haydn., Deformation rate effects on failure modes of open-cell Al foams and textile cellular materials, Int. J. Solids Struct. 43 (2006) 53-73.

30. C. Grabe, O.T. Bruhus, On the viscous and strain rate dependent behavior of plycrystalline NiTi, Int. J. Solids Struct. 45 (2008) 1876-1895.

31. Sanghaun Kimand Maenghyo Cho, A strain rate effect of Ni-Ti shape memory alloy wire, Jpn. J.Appl.Phys. 49(2010) 1-5.

32. D.P.Mondal, M.D.Goel and S. Das, Compressive deformation and energy absorption characteristics of closed cell aluminum-fly ash particle composite foam, Mater. Sci. Eng. A 507 (2009) 102-109.

33. M.D. Goel, D.P. Mondal, M.S. Yadav and S.K. Gupta, Effect of strain rate and relative density on compressive deformation behavior of aluminum cenosphere syntactic foam, Mater. Sci. Eng. A 590 (2014) 406-415.

[34] Z. Esen, S.Bor. Processing of Ti foam using magnesium space particle. Scripta Mater 2007;56:341-44.

[35] Changshu Xiang, Yan Zhang, Zengfeng Li. Preparation and compressive behavior of porous titanium prepared by space holder sintering process. Proc Eng 2012;27:768-74.

[36] Mondal DP, Majumdar Dutta J, Jha Nidhi, Badkul Anshul, Das S, Patel Aruna. Titanium-cenosphere syntactic foam made through powder metallurgy route. Mater Des 2012;34:82–9.

[37] A. Salimon, Y. Brechet, M.F. Ashby, A.L.Greer. Potential application for steel and titanium metal foams. J Mater Sci 2005;40:5793-99.

[38] Mansourighasri Amirhossein, Muhamad N, Sulong AB. Processing titanium foams using tapioca starch as a space holder. J Mater Proc Tech 2012;212(1):83–9.

[39] Wenjuan Niu, Chenguang Bai, GuiBao Qiu, Qiang Wang. Processing and properties of porous titanium using space holder technique. Mater Sci Eng A 2009;506:148–51.

[40] Andrews A, Sanders W, Gidson LJ. Compressive and tensile behaviour of aluminium foams. Mater Sci Eng A 1999;270:113–24.

[41] Shen Jianhu, Lu Guoxing, Ruan Dong. Compressive behaviour of closed cell aluminum foams at high strain rate. Compos Part B 2101; 41: 678–85.